

COMPARING MICROWAVE INDUCED POLYMERIZATION TO THERMAL
INDUCED POLYMERIZATION OF THE RESIN BISPHENOL A GLYCIDYL
METHACRYLATE.

by

Thomas Jerome Miller

Thesis submitted to the Faculty of the Graduate School of the
University of Maryland, College Park in partial fulfillment
of the requirements for the degree of
Master of Science
2004

Advisory Committee:

Professor Victor L. Granatstein, Chair
Senior Research Scientist Yuval Carmel
Professor Isabel Lloyd
Assistant Research Scientist Mark Walter

TABLE OF CONTENTS

Chapter I: Introduction.....	1
Chapter II: Theory of Polymers and Polymerization.....	4
Step Polymerization.....	4
Chain Polymerization.....	5
Degree of Conversion.....	7
Activation.....	10
Thermal Activation.....	10
Microwave Activation.....	12
Chapter III: Experimental Setup and Procedures.....	15
Resin.....	15
Sample Support.....	15
Microwave Source and Chamber.....	19
Microwave Simulations.....	21
Supplementary Setup.....	22
Pre-Cure Procedures.....	24
Curing Procedures.....	25
Post-Cure Procedures.....	26
Chapter IV: Data.....	27
Chapter V: Conclusions.....	36
Future work.....	37
References.....	38

CHAPTER I: INTRODUCTION

Polymerization is a chemical reaction where small molecules, called monomers, add together to make larger molecules, called polymers. This is interesting in many applications because while in monomer form, the material is fluid and can be molded into different shapes which then harden during polymerization [1]. Polymer materials are used in restorative dentistry as a binding material for creating replacement teeth. One example is bisphenol A-glycidyl methacrylate (bis-GMA) [2]. The purpose of this work is to compare microwave induced polymerization to thermal induced polymerization of bis-GMA.

The goal of restorative dentistry is to replace portions of degraded tooth structure. As a part of this goal, research has gone into identifying restorative materials that exhibit properties similar to tooth enamel, permanently bond to the tooth structure, initiate tissue repair, and esthetically match the tooth structure. The primary materials used are metals, ceramics, polymers, and composites [3]. Polymers and polymer based composites are of interest because they are aesthetically pleasing, inexpensive, and relatively easy to manipulate [4].

There are multiple methods of activating polymerization. Activation is the outside influence that causes polymerization to begin. Those most commonly used and studied for restorative dentistry are chemical, thermal, and light activation.

In chemical activation a catalyst is introduced. One example is tertiary amine and benzoyl peroxide. The tertiary amine catalyzes the chemical reaction that splits the benzoyl peroxide molecule into two free radicals [4]. One advantage of chemical activation is that it can occur at room temperature. Generally chemically activated resins polymerize less than those activated by other methods. This leads to less shrinkage, an additional advantage, but also leads to disadvantages. The unused monomer is a potential tissue irritant, and the less polymerized material is not as strong [5].

In heat activation, the monomer is heated until individual monomer molecules split into free radicals. One example is benzoyl peroxide [4]. When heated to between 50 to 100 Celcius the benzoyl peroxide splits into two free radicals that then initiate the polymerization. A problem that can occur in heat activation is if the monomer heats beyond its glass transition temperature. If heated above the glass transition temperature the thermal motion of the resulting polymer chains can prevent or overwhelm bonding, resulting in a weaker polymer [6]. The bis-GMA resin will begin to depolymerize between 125 and 200 degrees Celsius. Another disadvantage to heat polymerization is that it takes time. Typical durations for heat activation exceed thirty minutes [7], [8].

In light activation the monomer is exposed to a light source of a specific frequency. The frequency is chosen for direct absorption of energy into the monomer. An example is blue-green light with a wavelength of approximately 470 nm used to activate compounds such as camphorquinone and dimethylaminoethylmethacrylate that are added to the monomer [4]. The advantage to light activation is that it occurs faster than either heat or chemical activation. The primary disadvantage is sensitivity to color of the specimen [9]. The dentist needs to dye the replacement tooth structure to match the patient's teeth. This changes the index of refraction, and therefore the ability of the specimen to absorb light. It has been shown that lower intensities of light produce cured samples with lower degrees of conversion [10].

In microwave activation the sample is exposed to electromagnetic fields at microwave frequencies. Microwave activation occurs in times similar to that of light activation. Additionally, in preliminary investigations, Dr. Ivan Stangel, DDS of Biomat Sciences claims to have seen vastly improved strength and degree of conversion values for composite samples prepared via microwave [11]. He requested an explanation of the mechanism behind microwave interaction with bis-GMA, hence this work.

This work is organized as follows: Chapter II is on the theory of polymerization, describing the polymerization process and relating the macro-qualities of the resulting polymer to its degree of conversion. Chapter III will describe the experimental procedures and setups used to cure the samples, the equipment and testing procedures used to test the samples and the measurement of the data for this thesis. Chapter IV presents and discusses the experimental data. Chapter V presents the conclusions.

CHAPTER II: THEORY OF POLYMERS AND POLYMERIZATION

A polymer is a large molecule that is generated by linking together many smaller molecules. Polymerization is the name given to the process by which smaller molecules link to become polymers. There are two types of polymerization, step polymerization and chain polymerization. Step polymerization is also sometimes called condensation polymerization or step-growth polymerization. Chain polymerization is also sometimes called addition polymerization[12], [13].

STEP POLYMERIZATION

Historically, the first to be studied systematically was step polymerization. In step polymerization different compounds react to build a larger molecule with some by-products. An example is adipic acid and ethylene glycol. Figure 1 below shows a representation of their reaction. They form an ester link while generating a water molecule as a by product.

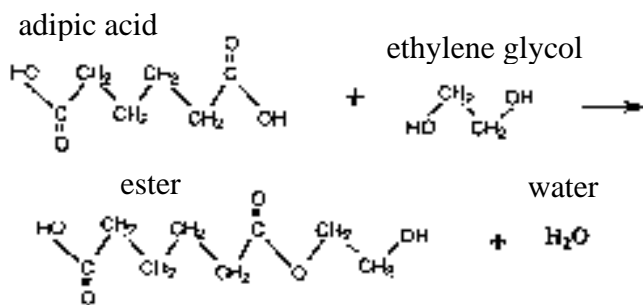


Figure 1: Adipic acid and ethylene glycol molecules react, creating an ester link and a water molecule.

The resulting molecule can continue to react with more adipic acid and ethylene glycol, making a long sequence of ester linkages and more water. As long as the numbers of adipic acid and ethylene glycol molecules are closely balanced, and the water is efficiently removed, the reaction will continue. Figure 2 below shows a representation of this.

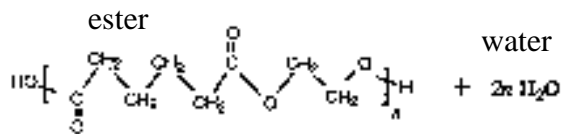


Figure 2: A long ester link with water. For each n sections of ester link, there are 2n molecules of water.

CHAIN POLYMERIZATION

In chain polymerization a monomer is split into free radicals, which react with other monomer molecules linking more and more of them together to create a polymer. Chain polymerization is what occurs with bis-GMA. Thus the free radicals are incorporated into the final polymer, and there are no byproducts in theory. In reality, byproducts can be generated. Chain polymerization can be divided into multiple stages. We will call these stages activation, propagation, and termination. We will follow the polymerization of tertiary butyl peroxide as an example.

To start activation, energy must be transferred into the monomer from an outside source. This energy is used to break some of the chemical bonds in the monomer, in our case a single bond between the two oxygens in the tertiary butyl peroxide molecule. This generates two free radicals, which are molecules that have an unpaired electron and therefore need to react chemically with another molecule in order to be stable.

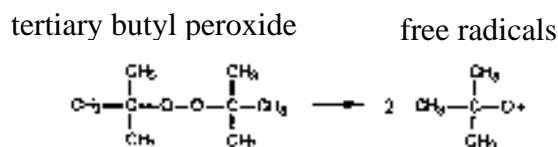


Figure 3: A tertiary butyl peroxide molecule is split in two.

The free radicals can then react with monomers such as styrene. This starts the polymer chain. Note that the polymer chain still contains an unpaired electron.

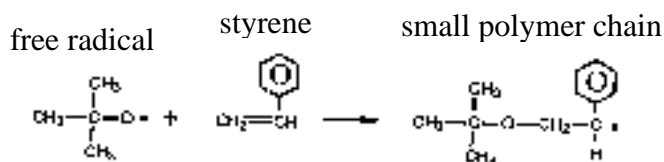


Figure 4: A free radical joins with styrene making a small polymer chain.

The unpaired electron at the end of the polymer chain causes the reaction to continue.

This is propagation.

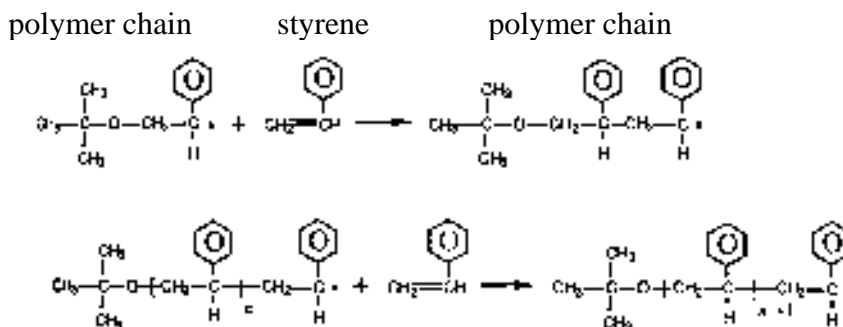


Figure 5: Smaller polymer chains join with styrene to make larger polymer chains.

Termination could theoretically occur when the source of monomers has been depleted. In most cases, termination results when the reactive portions of two chains join, making one long chain, otherwise called recombination. Less often disproportionation occurs, where a hydrogen atom is taken from one reactive chain to another forming two separate stable chains.

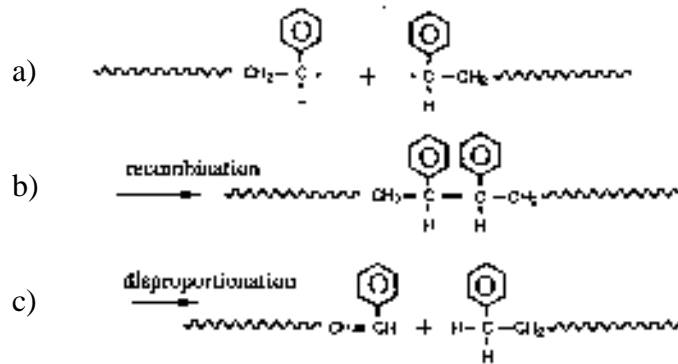


Figure 6: In a) two polymer chains approach each other. They may either b) undergo recombination or c) undergo disproportionation to stabilize and terminate the reaction.

DEGREE OF CONVERSION

Degree of polymerization, also called degree of conversion, refers to the percentage of monomers consumed during polymerization. This is used as an indicator of the thoroughness of polymerization and it has been shown that degree of conversion is the most important factor to examine for predicting final mechanical properties [14]. This coupled with the difficulties of using strength tests on samples to predict lifetime performance [15], [16] means that degree of conversion is indeed critical.

The higher the degree of polymerization, the stronger the polymer should be. To understand the underlying reason for this, it is necessary to talk about the strength of the covalent bonds. The strength of a covalent bond is defined as the energy required to break the bond. In methyl methacrylate polymerization, for example, double carbon bonds are split into two separate single carbon bonds.

In Figure 7 a) on the next page a growing polymer chain with an unpaired electron approaches a methyl methacrylate molecule. The double carbon bond, the C=C, splits into a single carbon bond and a free electron. Shown in Figure 7 b) the single carbon bond binds the methyl methacrylate to the growing polymer chain, and the free electron seeks out additional methyl methacrylate with which to interact. The energy change during a chemical reaction is the difference between the initial bond energy and the final bond energy.

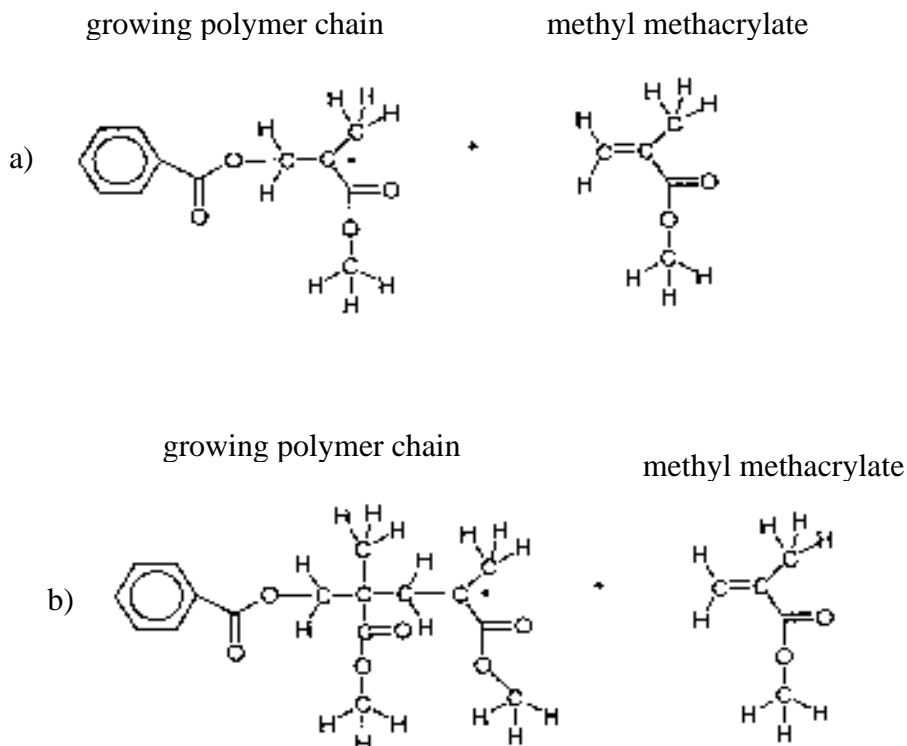


Figure 7: Methyl methacrylate polymerization.

The energy change of a single monomer being incorporated into the growing polymer chain is:

$$\Delta E = \Sigma(\text{bond energies of broken bonds}) - \Sigma(\text{bond energies of created bonds})$$

$$\Delta E = \Sigma(614 \text{ kJ}) - \Sigma(348 \text{ kJ})$$

$$\Delta E = 266 \text{ kJ}$$

Exothermic reactions create bond combinations that are stronger than the initially broken bonds. The energy that creates the stronger bonds and is shed thermally during the reaction comes from the molecule's electrons, which drop to lower energy orbits during the process. The greater the degree of polymerization, the greater the number of bonds generated. This translates to larger polymer chains. Therefore a polymer with a higher degree of conversion should require more energy to break than a polymer with a lesser degree of conversion.

Some practical factors can cause problems. Sometimes cross-linking occurs between different polymer chains, increasing the strength of the resulting polymer even further. The stress of the chemical reaction also occasionally causes cracks in the polymer, weakening it. Therefore the degree of conversion relates to the macro properties of the polymer only if the process is carefully controlled.

ACTIVATION

Activation requires an initial input of energy to the monomer from an external source. This energy splits some of the monomer molecules into free radicals, which then polymerize the material. Once activation begins, the polymerization is exothermic and the process completes without additional energy input. Work by Musanje and Darvell [17] suggests that additional energy input after activation begins will not improve results.

The activation choices for restorative dentistry are chemical, light, thermal, and microwave. This work focuses specifically on experimental comparison of thermal and microwave activation for the bis-GMA resin.

THERMAL ACTIVATION

Thermal transfer of energy occurs in three ways, radiation, conduction, and convection. Radiation is the direct transfer of energy from the source to the object. Conduction is the transfer of energy to the object through an interim material that may be solid, gas, or liquid. Convection is the transfer of energy from a solid source or object to a moving mass of liquid or gas [18]. To an extent we have all three occurring.

Equation 1 details energy transfer per unit time for radiation.

$$dQ/dt = eA\sigma(T_s - T_o)^4 \quad (1)$$

'e' is the emissivity of the object. Emissivity is a measure of efficiency for thermal transfer of energy in to and out of the object. It can take values from 0 to 1, with one being the emissivity of a perfect or blackbody emitter. 'A' is the surface area of the object. ' σ ' is the Steffan-Boltzmann constant, $5.67 \times 10^{-8} \text{ W/m}^2\text{K}^4$ in SI units. ' T_s ' is the temperature in degrees Kelvin of the source and ' T_o ' is the temperature in degrees Kelvin

of the object. If $T_s > T_o$ the object is receiving energy, if $T_s < T_o$ the object is giving off energy, and if $T_s = T_o$ no energy is transferred.

Equation 2 details energy transfer per unit time for conduction.

$$dQ/dt = cA(T_s - T_o)/L \quad (2)$$

'c' is the thermal conductivity of the material between the object and the source. For acrylic, which bis-GMA is, $c = 0.01 \text{ W/mK}$ [19]. 'A' is again the surface area of the object. 'L' is the distance between the object and the source. Again ' T_s ' is the temperature in degrees Kelvin of the source and ' T_o ' is the temperature in degrees Kelvin of the object.

There are no simple equations for describing convection. Heated air near the heating elements or the thermal setup will want to rise while cooler air away from the heating elements will fall. A detailed understanding of the air turbulence induced would be involved, uncertain, and unnecessary for the completion of this work. The effect of convection can be minimized experimentally by preheating the thermal chamber prior to inserting the sample.

$$\partial T / \partial t = k \nabla^2 T \quad (3)$$

Distribution of temperature within a solid sample is governed by the diffusion equation. In equation 3 'T' is the temperature of the sample, 'k' is the diffusion coefficient and 't' is time. For polymethylmethacrylate, which bis-GMA is, $k = 1.24 \times 10^{-6} \text{ m}^2/\text{s}$ [20].

MICROWAVE ACTIVATION

In the case of microwave activation, energy transfer is due to interaction of the material and the electromagnetic field. Microwave energy transfer in a microwave oven is typically higher than thermal energy transfer in a thermal oven. Work by Halverson et al. [21] has related rate of energy transfer to extent of polymerization, meaning microwave activation should have an advantage over thermal activation. Depending on the properties of the material, the wave will penetrate the sample and deposit energy. In this way, using microwave activation may deposit energy more evenly than thermal activation would. We start with the wave equation [22], [23]:

$$\nabla^2 \mathbf{E} - \mu \epsilon \partial^2 \mathbf{E} / \partial t^2 = 0 \quad (4)$$

' \mathbf{E} ' is the electric field vector, ' μ ' is the magnetic permeability of the material and ' ϵ ' is the electric permittivity of the material. The wave is generated at the source, in the case of this work, a magnetron, with sinusoidal varying time component:

$$E \propto E_0 e^{-i\omega t} \quad (5)$$

Where ' E ' is the electric field, ' E_0 ' is the magnitude of the electric field in V/m, ' ω ' is the frequency of oscillation in 2π Hz, and ' t ' is the time in seconds. Inserting Equation 5 into Equation 4 leads to:

$$\nabla^2 \mathbf{E} + \mu \epsilon \omega^2 \mathbf{E} = 0 \quad (6)$$

This can be simplified due to the fact that choice of the microwave chamber can constrict the electric field to only being polarized in one direction and propagating in another.

Choosing the polarization direction unit vector as \mathbf{x}_0 and the propagation direction unit vector as \mathbf{z}_0 gives:

$$\partial^2 E_x / \partial z^2 + \mu \epsilon \omega^2 E_x = 0 \quad (7)$$

Solving Equation 7 gives the electric field equation:

$$E_x = E_0 e^{-i\omega t} e^{-ikz} \quad (8)$$

Where $k = \omega(\mu\epsilon)^{1/2}$. Because the magnetic and electric fields are coupled, the magnetic field is:

$$H_y = H_0 e^{-i\omega t} e^{-ikz} \quad (9)$$

Where ' H_y ' is the magnetic field in the \mathbf{y}_0 unit vector direction, and ' H_0 ' is the magnitude of the magnetic field. To solve for the power within the fields, and also for the energy transfer from the fields to the material, it is necessary to calculate the Poynting vector:

$$\mathbf{S} = \mathbf{E} \times \mathbf{H}$$

Where ' \mathbf{S} ' is the vector of the power flux in Watts/meters², ' \mathbf{E} ' is the electric field vector and ' \mathbf{H} ' is the magnetic field vector. It is useful to show another relation between the electric and magnetic fields using Maxwell's equations, specifically:

$$\nabla \times \mathbf{E} = - \partial \mathbf{B} / \partial t$$

We can show, for the solutions to E_x and H_y that we have:

$$- (\mu\epsilon)^{1/2} E_x = B_y \quad (10)$$

Therefore, the Poynting vector becomes:

$$\mathbf{S} = - \mathbf{z}_0 (E_x)^2 (\mu\epsilon)^{1/2} (\mu)^{-1} \quad (11)$$

$$\mathbf{S} = - \mathbf{z}_0 (E_0 e^{-i\omega t} e^{-ikz})^2 (\epsilon/\mu)^{1/2} \quad (12)$$

The time average of this is:

$$\mathbf{S} = - \mathbf{z}_0 (1/2) (E_0 e^{-ikz})^2 (\epsilon/\mu)^{1/2} \quad (13)$$

Inside the material the electric permittivity and permeability are complex functions of the frequency. Substituting $\epsilon = (\epsilon' - i\epsilon'')\epsilon_0$ into $k = \omega(\mu\epsilon)^{1/2}$ leads to:

$$\mathbf{S}_{\text{ave}} = -\mathbf{z}_0(1/2)(E_0)^2(\epsilon/\mu)^{1/2}\exp[-i2z\omega(\mu(\epsilon' - i\epsilon'')\epsilon_0)^{1/2}] \quad (14)$$

Where ϵ' is the real part of ϵ , ϵ'' is the imaginary part of ϵ , the value of ϵ in freespace is $\epsilon_0 = 8.854 \times 10^{-12} \text{ C}^2/\text{Nm}^2$, and $\exp(x) = e^x$. Now, with a little more math and using the expression for the loss tangent $\delta = \epsilon''/\epsilon'$:

$$\begin{aligned} \mathbf{S} = & -\mathbf{z}_0(1/2)(E_0)^2(\epsilon/\mu)^{1/2}\exp[-2z\omega\{(\mu\epsilon'\epsilon_0/2)((1+\delta^2)^{1/2}-1)\}^{1/2}] \\ & \times \exp[-i2z\omega\{(\mu\epsilon'\epsilon_0/2)((1+\delta^2)^{1/2}+1)\}^{1/2}] \end{aligned} \quad (15)$$

So we can see that the power density in the field decreases as $\exp[-2z\omega\{(\mu\epsilon'\epsilon_0/2)((1+\delta^2)^{1/2}-1)\}^{1/2}]$. This implies that the material is absorbing the energy. How deeply the wave deposits energy is dependent on δ . For bis-GMA, $\delta = 0.119$, and $\epsilon' = 4.2$, for $\omega = 2\pi \times 2.45 \text{ GHz}$, and μ is assumed as $\mu = \mu_0 = 4\pi \times 10^{-7} \text{ W/Am}$. Therefore the skin depth, defined as the depth at which the power flux has dropped off to a factor of $1/e$, is calculated to be 0.080 m .

CHAPTER III: EXPERIMENTAL SETUP AND PROCEDURES

Figure 8 below depicts a block diagram of the setup. Solid arrows represent flow of microwave energy, and the dashed line represents the temperature sensor. Microwave energy emanating from the source passes through a circulator to the microwave chamber. In the microwave chamber the energy is applied to the sample which is within the sample support. Any reflected energy is redirected by the circulator to the load. The temperature reader collects the data from the temperature sensor, which penetrates the microwave chamber and comes into contact with the sample.

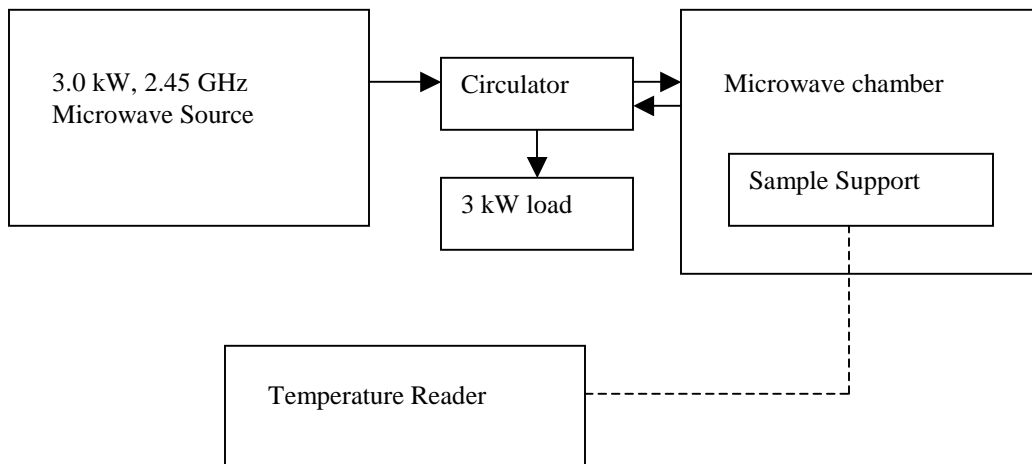


Figure 8: Block diagram of the setup.

RESIN

The resin used to make the sample during testing was provided by Biomat Sciences. It was specifically formulated for thermal curing, designated Biomat Resin "A", prepared on 07-16-01 and consisting of 74.75 % weight bis-GMA, 24.75 % weight tri-ethylene glycol dimethacrylate (TEGDMA) which reduces the viscosity of the mixture, and 0.5 % weight Benzoyl Peroxide (BPO) which is the initiator [11].

Composite material tested was also provided by Biomat Sciences and included 25% weight resin as described above and 75% weight Alumina filler [11].

SAMPLE SUPPORT

The direct sample support structures were constructed from teflon, which was chosen for its low loss tangent $\delta \sim 0.0001$. Three parts, the bar mold, the bar mold support and the bar mold guide are pictured in figures 8, 9, and 10 below.

Figure 9 is the bar mold. The purpose of the bar mold is to contain the liquid resin in the shape required for the cured samples. For 3-point flexural strength tests the samples prepared needed to be 25 by 2 by 2 mm³.

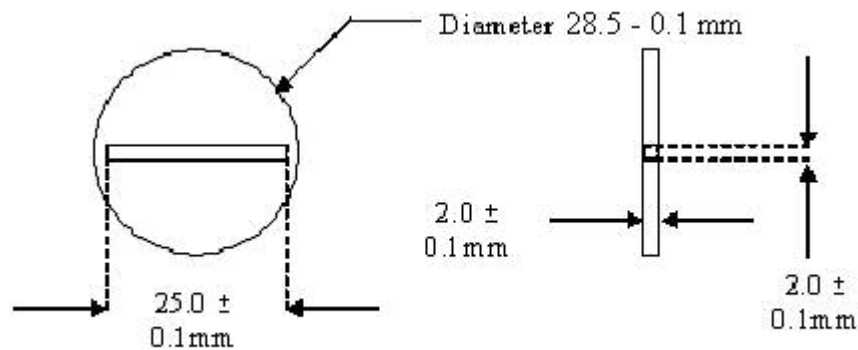


Figure 9: Mechanical drawing of the bar mold

Figure 10 is the bar mold support. The purpose of the bar mold support is to raise the bar mold to the center of the microwave chamber. Since the microwave chamber is based on WR284 waveguide, the interior dimensions are 72.1 by 34.0 mm. The 17.0 mm height of the bar mold support is half of the 34.0 mm dimension of the Microwave Chamber. The 28.5 mm diameter of the bar mold support was chosen to match the 28.5 mm diameter of the bar mold. The 3.2 mm diameter hole through the center of the bar mold support allows access for a thermal sensor to the center of the sample during curing.

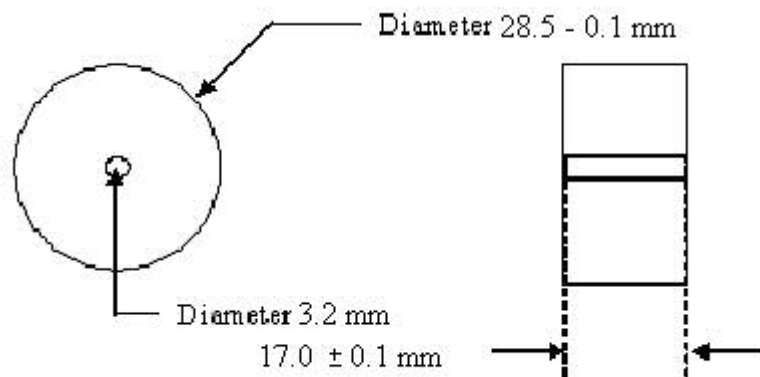


Figure 10: Mechanical drawing of the bar mold support.

Figure 11 is the bar mold guide. The purpose of the bar mold guide is to hold the bar mold and bar mold support in position with relation to each other and the microwave chamber and the plug. The 28.5 mm inner diameter was chosen to match the bar mold and bar mold guide. The 31.8 mm outer diameter was chosen to be less than the access hole in the microwave chamber.

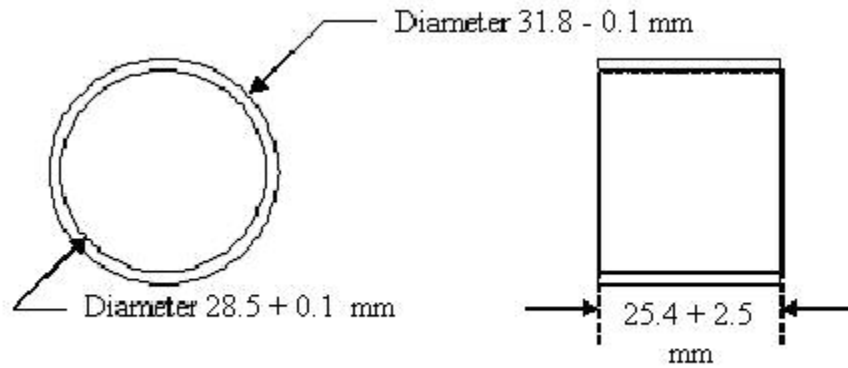


Figure 11: Mechanical drawing of the bar mold guide

Figure 12 is an assembly drawing of the bar mold, bar mold support and bar mold guide. This is the sample support. This assembly is inserted into the microwave chamber on the plug pictured in figure 13.

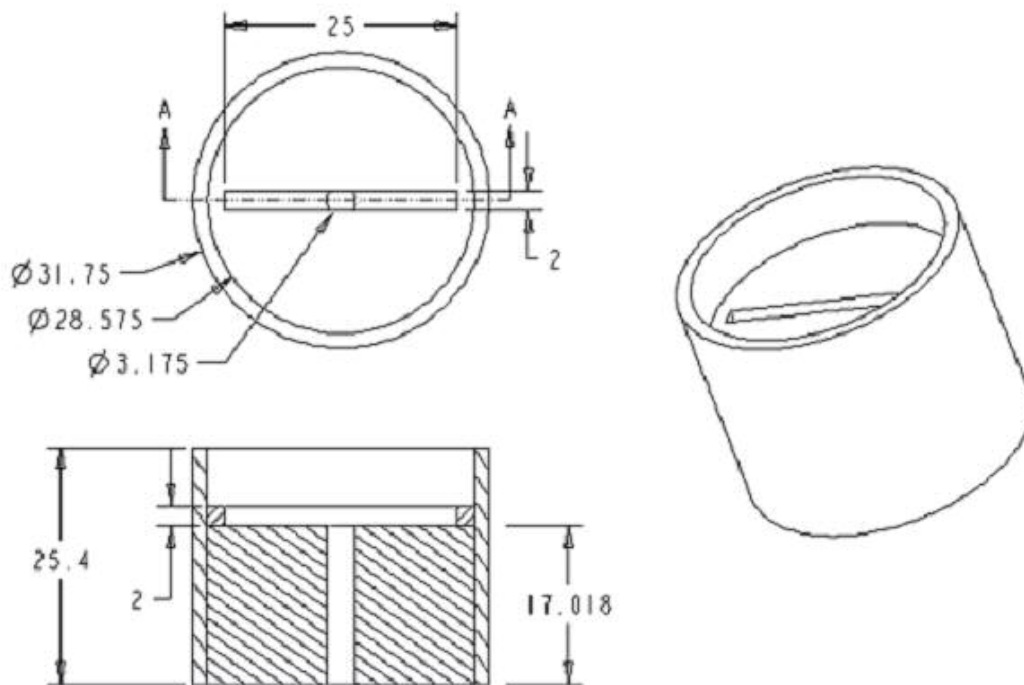


Figure 12: Assembly drawing of the bar mold, bar mold support and bar mold guide. All dimensions are mm.

MICROWAVE SOURCE AND CHAMBER

The microwave source used was a Microwave Materials Technologies 3.0 kW 2.450 GHz source driving the TE₁₀ mode into a WR284 waveguide output. It is continually adjustable from 0.00 - 3.00 kW output with a forward and reflected power measurement accuracy of ± 0.05 kW.

The Microwave Chamber was constructed from a 0.2312 m (9.113 inch, one waveguide wavelength) of WR284 copper waveguide with two CMR284 flanges, and is pictured in figure 13 below. The 57.9 mm distance from the end is one quarter waveguide wavelength for 2.45 GHz in WR284 waveguide. This places the center of the 38.1 mm access hole at a field power peak in the TE₁₀ mode. The 38.1 mm distance from the edge centers the 38.1 mm access hole.

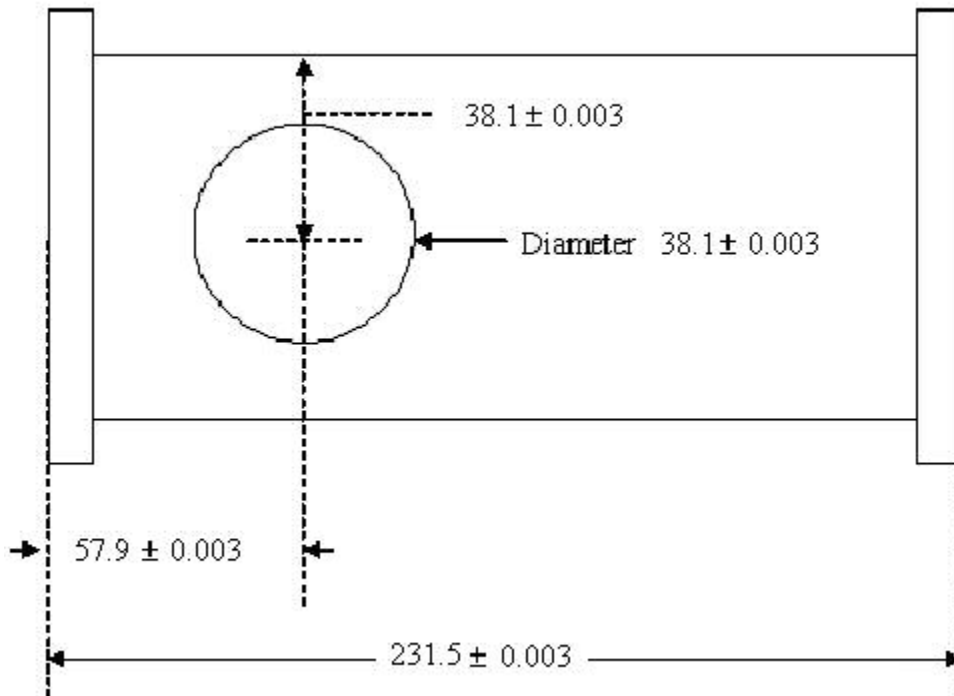


Figure 13: Mechanical drawing of the microwave chamber. Dimensions are mm.

The hole for inserting the sample consistently into an area of peak field strength was filled during tests with a plug which is pictured in figure 14. The 50.8 mm diameter of the plug was chosen to be larger than the 38.1 mm diameter of the access hole. The 28.5 mm diameter raised portion of the plug was chosen to match the bar mold, bar mold support and bar mold guide. The 3.2 mm hole allows access for a thermal sensor to the sample. The 2.0 mm height of the raised portion of the plug matches the 2.0 mm thickness of the wall of the microwave chamber. The plug was constructed from brass to maintain electrical contact with the copper microwave chamber.

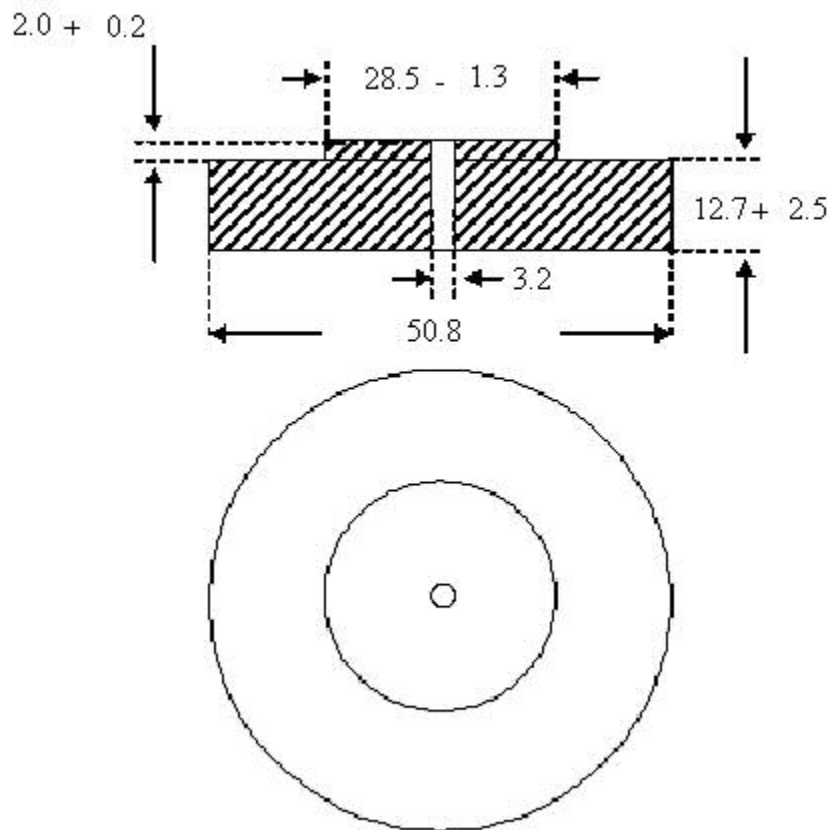


Figure 14: Mechanical drawing of the plug. Dimensions are in mm.

MICROWAVE SIMULATIONS

Simulations run in Hewlett-Packard High Frequency Structure Simulator (HP HFSS) confirmed the predicted field strength locations and results are pictured in figure 15, and 16 below. Figure 15 is a simulation of half of the microwave chamber. The right side is a port for input and output of energy, and all other walls are perfect conductors. In the center is the teflon support with a resin sample. The lines inside the chamber represent relative E field strengths, the darkest in the center representing peak field strength. Performing the simulation on half of the microwave chamber allows HP HFSS to concentrate on a smaller area, without significantly changing the results.

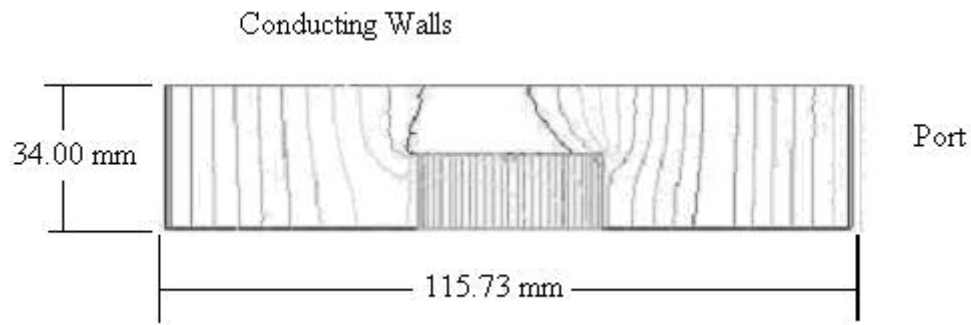


Figure 15: Half microwave chamber HP HFSS simulation.

Figure 16 is a simulation of one quarter of the microwave chamber. The right side is a port for input and output of energy, bottom is a symmetry plan, and all other sides are perfect conductors. The lines inside the chamber represent relative E field strength, with the strongest being the darkest lines near the sample holder. The E field is symmetric about the center axis, which allows the use of the symmetry plane. Making use of symmetry planes allows for faster and more accurate simulation.

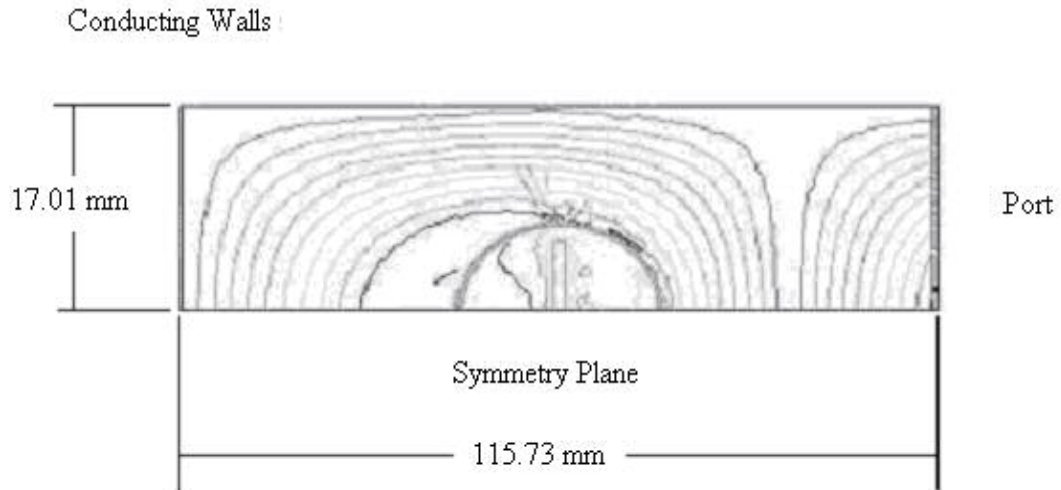


Figure 16: HP HFSS simulation with symmetry plane.

SUPPLEMENTARY SETUP

Thermal curing was conducted in a GE model XL44 home convection oven.

Temperature was measured using a T-type thermocouple and HP thermocouple reader.

Temperature measurement and recording during curing was performed with Fiso Technologies model FOT-HERO fiber optic sensors in conjunction with model TM-250 sensor reader. The FOT-HERO sensors were rated for 0 - 200⁰ Celcius with an accuracy of $\pm 1.0^0$ C. The FOT-HERO consists of a Fabry-Perot cavity at the end of a fiber optic cable. This chamber is broad band illuminated, and the resonant frequency of the chamber varies as the chamber expands and contracts due to temperature variations. An FOT-HERO is pictured in figure 17.

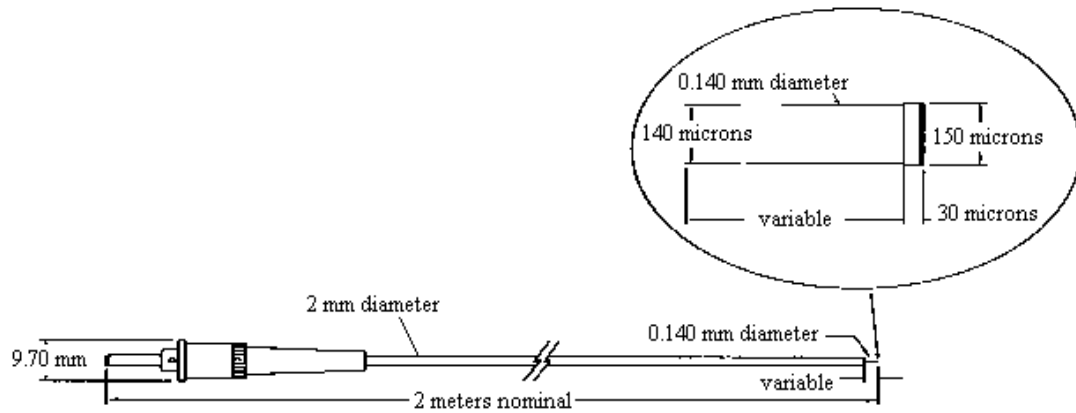


Figure 17: FOT-HERO

The mechanical test performed post curing was three point flexural strength testing using an Instron Universal Electromechanical Tester model 4465 with load measurement accuracy of $\pm 0.5\%$, and head position accuracy of ± 0.02 mm. A diagram of the test is depicted in figure 18. Force is applied to the center of the sample which is supported at the ends. The force, in N, required to break the sample is recorded and used with the dimensions of the sample to calculate the strength in MPa. For the test to be accurate, the samples must be close to $2 \times 2 \times 25 \text{ mm}^3$ in dimension.

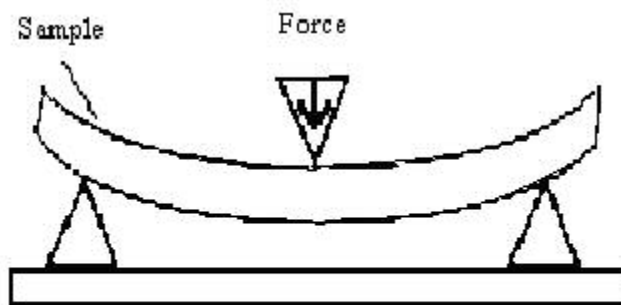


Figure 18: 3-point flexural strength testing.

Fourier Transform Infrared (FTIR) analysis for degree of conversion (DOC) was carried out using an Excalibur Series BioRad FTS 3000. FTIR works by launching infrared energy at the sample and recording the energy/wavelength scattering from the sample. Each wavelength corresponds to a different portion of the molecular structure. 1640 nm is the wavelength of interest for double carbon bonds. DOC is then calculated by:

$$1 - R = \text{DOC}$$

Where R is the ratio of the area under the peak at wavelength 1640 nm prior to and post curing.

PRE-CURE PROCEDURES

When not in use, the test resin was wrapped in a paper bag and stored in a refrigerator at 45 Fahrenheit. At all times latex gloves were worn to prevent direct skin contact with the sample, and to prevent contamination of the sample.

When it was time to conduct tests the resin was removed from the refrigerator and allowed to sit at room temperature for a minimum of 20 minutes. One side of the bar mold would then be covered with scotch tape to prevent the resin from seeping out the bottom. The resin was then inserted into the bar mold using a plastic syringe. The resin would be allowed to sit for an additional 20 minutes to allow any air bubbles introduced to escape.

The top of the bar mold would then be covered with scotch tape in order to prevent air-inhibition of the polymerization. The bar mold would then be placed on the bar support and both inserted into the bar guide. All three of which would then be placed on the plug. The plug was then inserted into the microwave chamber, with the sample aligned so that its 25 mm axis ran parallel to the 76.2 mm axis of the WR284 waveguide.

The plug was then clamped in place using two clamps. Finally, if being used, the Fiso temperature sensor would be inserted through the 3.2 mm diameter access hole in the Plug until in contact with the center of the bar mold, separated from the resin by the Scotch Tape. 3M copper tape was then used to seal the access hole to prevent escape of microwave energy.

CURING PROCEDURES

Prior to beginning experiments, the microwave run with no sample in place as forward and reflected power measurement calibration. The manual dial setting would then be left in place.

Once the process for pre-curing was complete, the clock in the laboratory was used to time the duration of test. During the time that the microwave source was on, a NARDA model 8712 Electric Radiation Survey Meter with model 8723D Isotropic Electric Field Probe was used to measure for leakage of microwave energy in the area within 1 foot of the microwave chamber for safety reasons. Once the test was complete, the sample would be removed from the microwave chamber and allowed to sit at room temperature for 20 minutes before being removed from the bar mold. The bar mold would be allowed to rest at room temperature for at least an hour before re-use.

POST-CURE PROCEDURES

Once a cured sample was removed from the bar mold it would be inserted into a non-reactive food quality 1 oz. opaque container and placed in the freezer at 10 Fahrenheit. Once removed from the freezer it would be placed into a cooler and taken to Biomat Sciences for mechanical evaluation within 24 hours. At Biomat Sciences the samples would be measured for exact dimensions then processed for flexural strength and degree of conversion.

CHAPTER IV: DATA

Prior to comparing microwave results to other methods, experiments were performed to optimize microwave curing. Power and duration of microwave exposure were checked. For this work, primarily 1.0 kW and 0.5 kW were studied. Figure 19 below compares degree of conversion for samples prepared at 0.5 kW for 30 s to samples prepared at 1.0 kW for 15 s. Nine samples were prepared at 0.5 kW for 30 s and four were prepared at 1.0 kW for 15 s. For samples prepared at 0.5 kW the mean equals 0.869 and the standard deviation equals 0.196. For samples prepared at 1.0 kW the mean equals 0.746 and standard deviation equals 0.089.

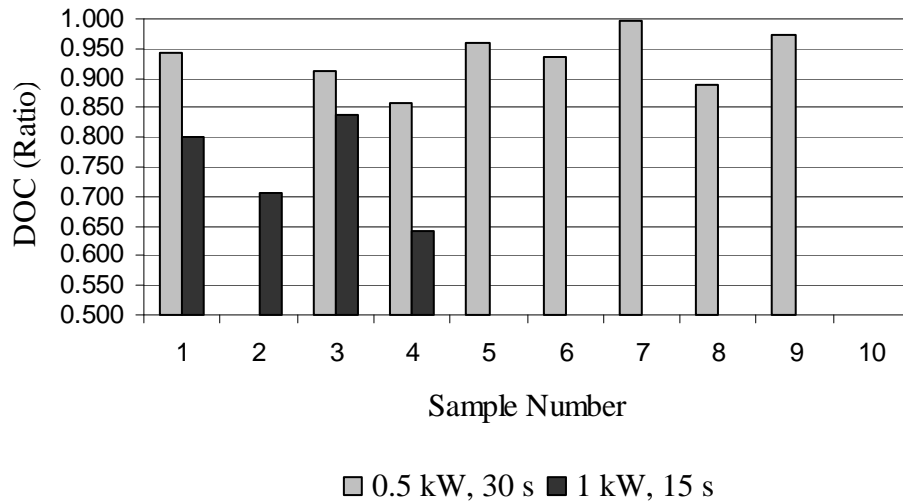


Figure 19: Degree of conversion versus microwave power.

Figure 20 compares flexural strength of 0.5 kW, 30 s to 1.0 kW, 15 s. Note the direct relation of degree of conversion to flexural strength. For the samples prepared at 0.5 kW the mean equals 60.29 MPa and the standard deviation equals 22.02. For the samples prepared at 1.0 kW the mean equals 29.44 MPa and the standard deviation equals 8.97.

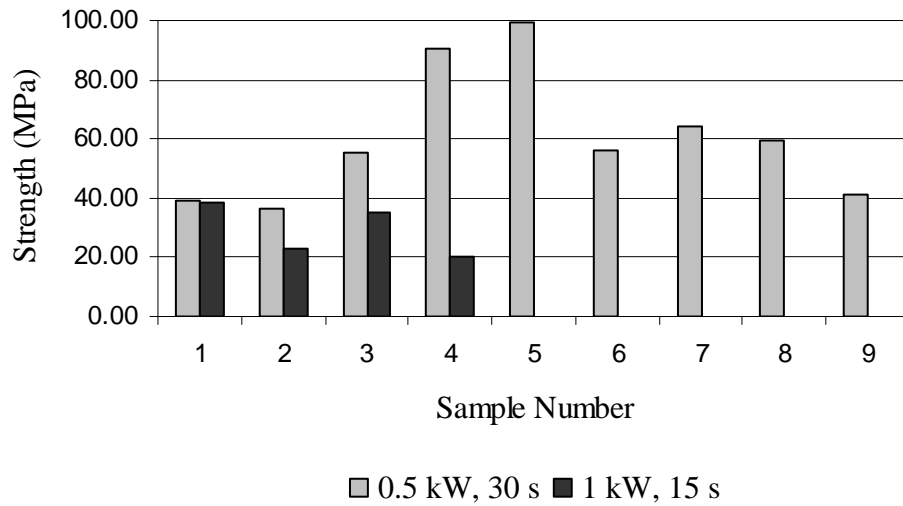


Figure 20: Flexural strength versus microwave power.

Next time spent in microwave was explored. Figure 21 compares degree of conversion for samples prepared at 120 s and 30 s. Note that there is no improvement in degree of conversion from the prolonged exposure. Again, for the nine samples prepared at 0.5 kW, 30s the mean equals 0.869 and the standard deviation equals 0.196. For the eight samples exposed to 0.5 kW for 120 s, the mean equals 0.915 and the standard deviation equals 0.047.

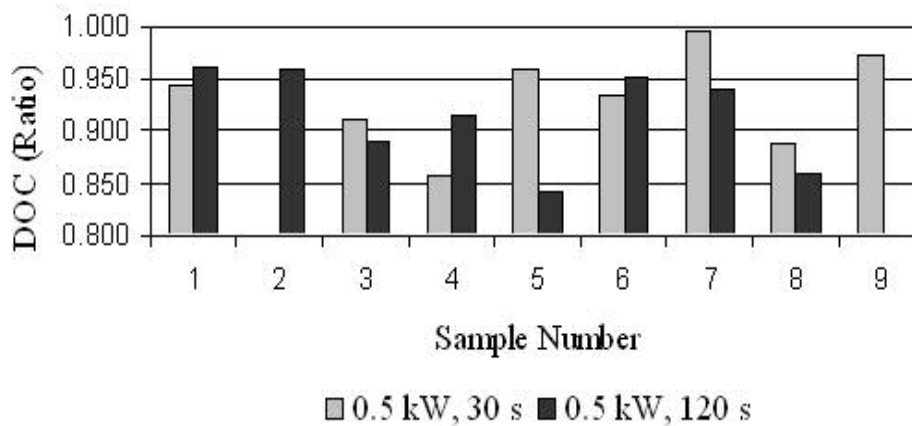


Figure 21: Degree of conversion versus microwave duration.

Figure 22 compares flexural strength of samples prepared at 0.5 kW for 30 s and for 120 s. Only three of the eight samples prepared for 120 s were suitable for mechanical testing. The other five emerged from the curing process fractured. For the three samples from 120 s exposure that were tested, the mean equals 30.49 MPa and the standard deviation equals 13.95. This is much lower than the mean of 60.29 MPa and standard deviation of 22.02 for samples exposed for 30 s.

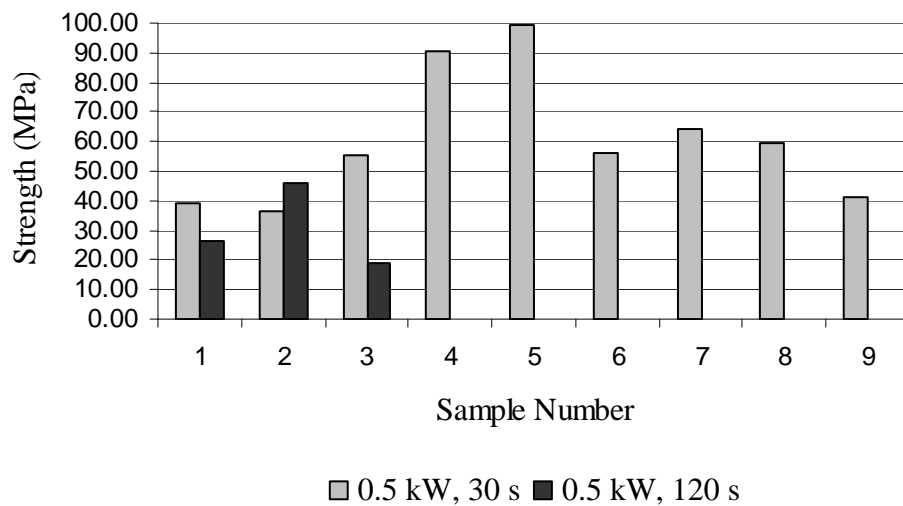


Figure 22: Flexural strength versus microwave duration.

Figure 23 compares degree of conversion for different processing methods. Literature is per work by Bartoloni, et al [24], and includes values for thermal, light, and microwave curing.

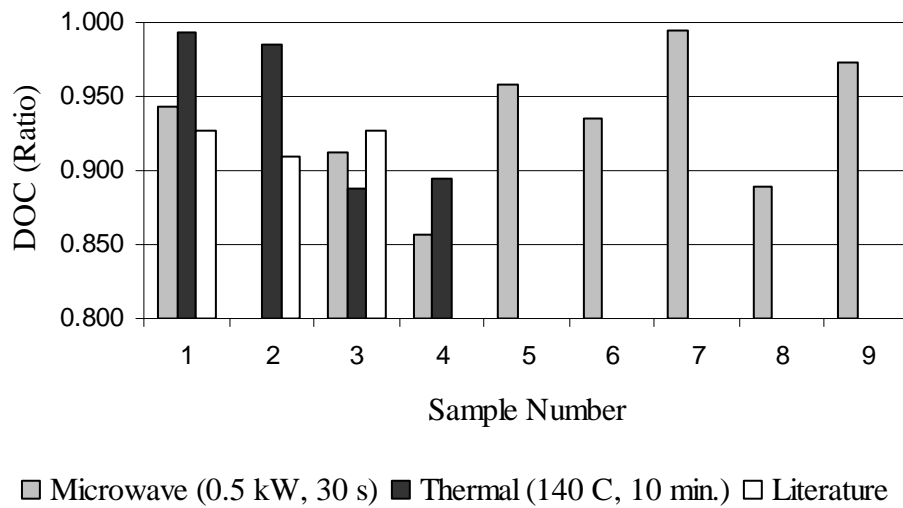


Figure 23: Degree of conversion by method of cure.

Figure 24 compares flexural strength of several different methods. The literature is per Tam et al. [25], and Smith et al. [26], and includes values for thermal, light, and microwave curing. Only three of the eight samples prepared at 140 C, 10 min. were suitable for mechanical testing. The other five emerged from the curing process fractured. For those three samples, the mean equals 135.90 MPa with a standard deviation of 19.93.

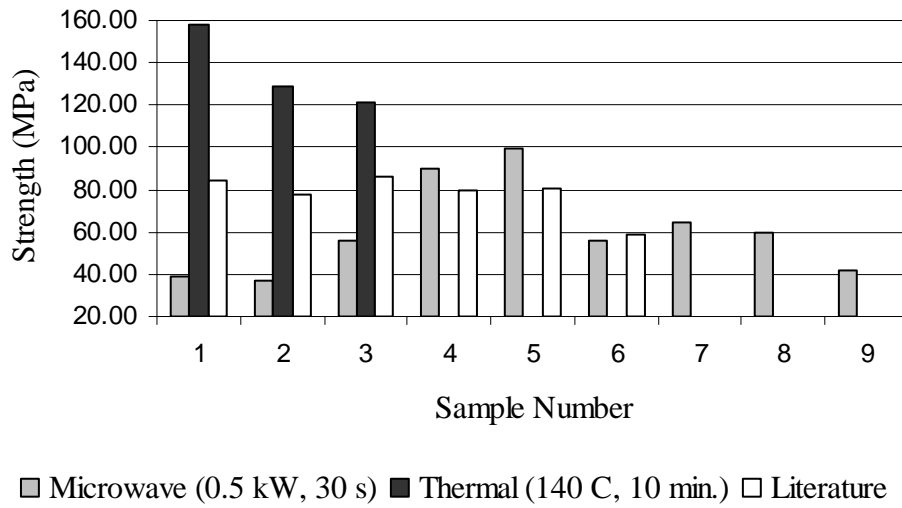


Figure 24: Flexural strength versus method of cure.

Figure 25 shows the temperature rise of a 0.500 in. diameter by 0.125 in. thick sample of bis-GMA during 0.5 kW microwave processing. The microwave was turned on at $t = 0$ s, and polymerization starts at approximately $t = 15$ s, once the sample reached ~ 130 C. This is interesting because 130 C is the thermal activation temperature.

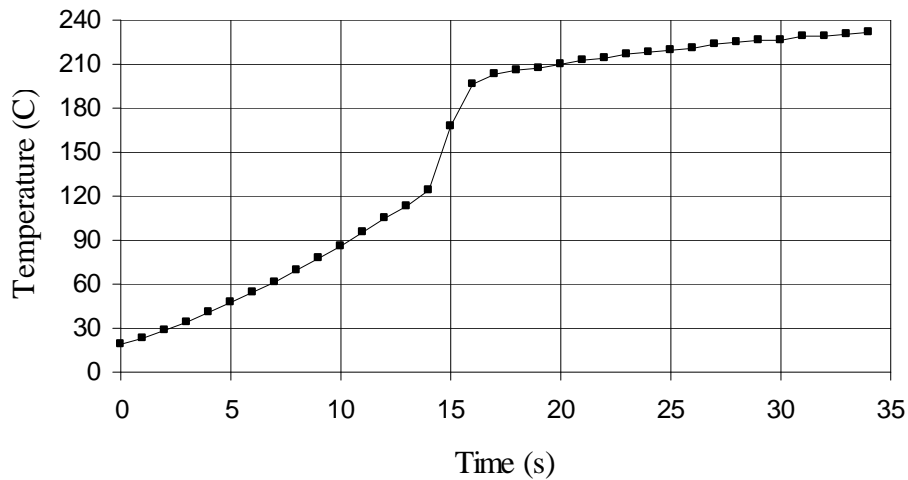


Figure 25: Temperature rise, resin only, 0.5 kW.

Figure 26 shows the derivative of the temperature rise shown in Figure 25. Note the sharp change in rate of temperature rise once polymerization initiates at about $t = 14$ s. This is due to the exothermic nature of the reaction. From $t = 14$ s to $t = 16$ s we have the temperature rise due to the exothermic polymerization. Afterwards the profile returns to a linear profile due to microwave input. The change in the temperature rise slope from before to post polymerization indicates that the complex dielectric values for polymerized bis-GMA differ from the prepolymerization values.

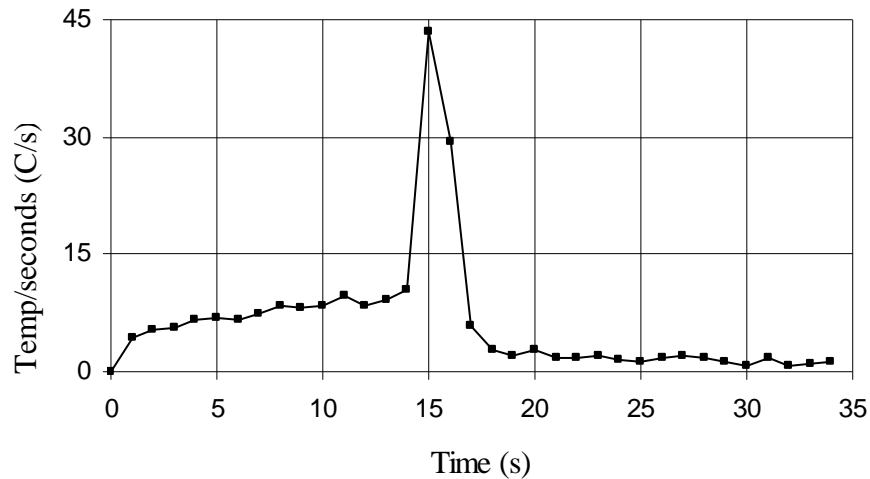


Figure 26: Temperature rise derivative, resin only, 0.5 kW.

Figure 27 shows the temperature rise of a 12.7 mm diameter by 3.2 mm thick sample of bis-GMA during 0.1 kW microwave processing. The microwave was turned on at $t = 0$ s, and polymerization starts at approximately $t = 85$ s, once the sample reached ~ 130 C. Therefore, at two different microwave power settings, polymerization began only after the resin achieved thermal activation temperature. Again, note that the temperature rise slope prior to $t = 14$ is different from that after $t = 16$.

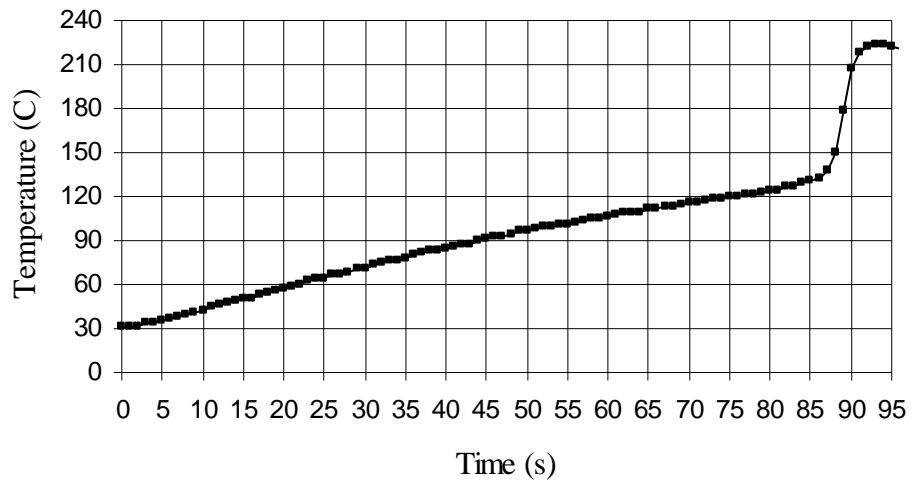


Figure 27: Temperature rise, resin only, 0.1 kW.

Figure 28 shows the derivative of the temperature rise shown in Figure 27. Note that there is a sharp change in rate of temperature rise once polymerization initiates at about $t = 85$ s. This is due to the exothermic nature of the chemical reaction.

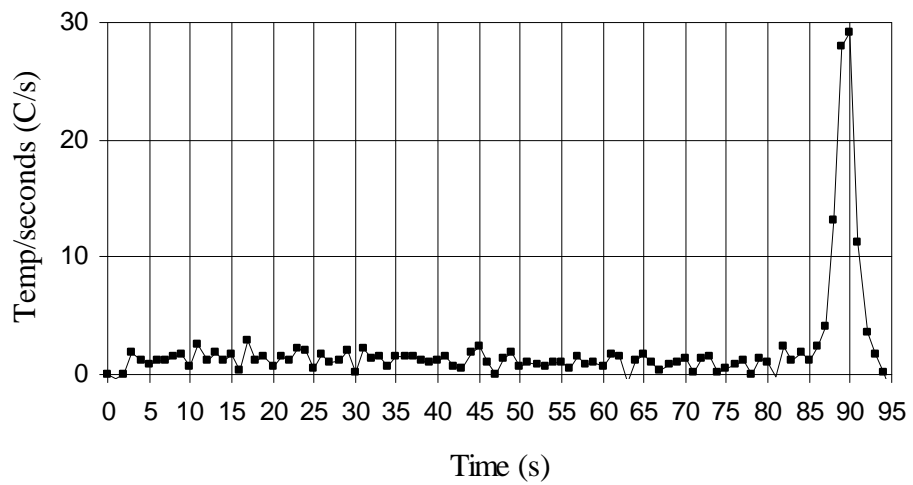


Figure 28: Temperature rise derivative, resin only, 0.1 kW.

Figure 29 shows the temperature rise of a 0.500 in. diameter by 0.125 in. thick sample of composite resin during 0.5 kW microwave processing. Note that the profile of the temperature rise is very different from that for resin alone. This indicates that the addition of the filler has a significant impact on microwave induced polymerization.

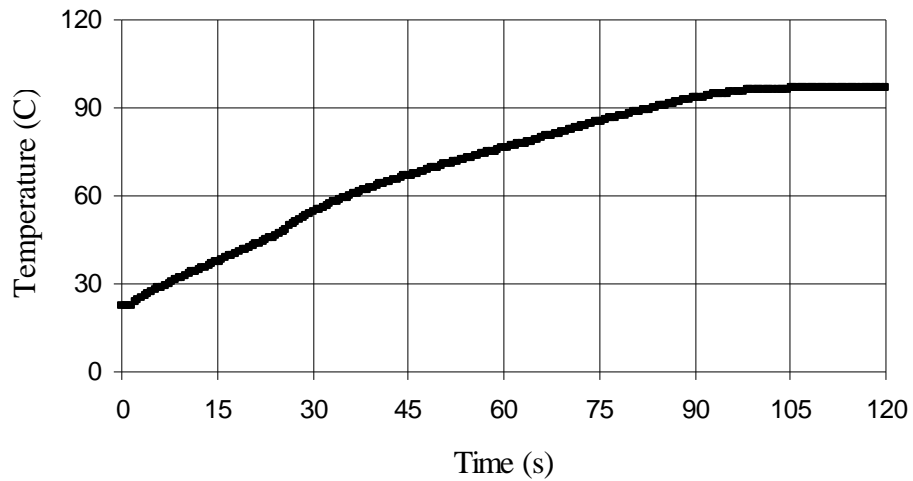


Figure 29: Temperature rise, composite, 0.5 kW.

Figure 30 shows the derivative of the temperature rise shown in Figure 29. Note that the slope of the temperature rise is also significantly different from that for resin alone. There is no sharp spike showing exactly when polymerization began. Most likely polymerization began just before $t = 30$, where there is a peak in the temperature rise.

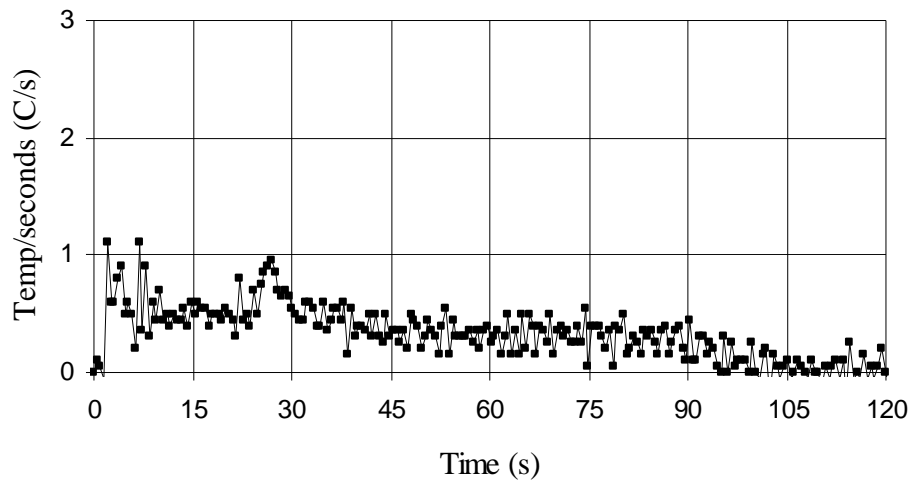


Figure 30: Temperature rise derivative, composite, 0.5 kW.

CHAPTER V: CONCLUSIONS

Based on the data obtained, microwave initiated polymerization is brought about by microwave heating of the bis-GMA. Additionally, microwave initiated polymerization takes a fraction of the time required to bring about thermal initiated polymerization. Therefore the initial results obtained by Biomat Sciences with composite material are due to mixed interaction of microwave energy, resin, and filler material.

The conclusion that microwave initiated polymerization is microwave heating and not a different mechanism is based on comparing degree of conversion of the samples prepared, strength of the samples prepared, and temperature at which activation occurs. If microwave activation were a different mechanism than thermal activation, it would have been expected that these parameters would have had dissimilar results. However, degree of conversion, flexural strength, and temperature of activation for microwave cured samples did not differ significantly from thermally cured samples or from available data in literature.

The significant differences in temperature rise profiles for bis-GMA alone versus bis-GMA mixed with alumina indicate that the addition of the alumina has a significant impact on the process. This can be explained by the differences in the complex permittivity values for bis-GMA and alumina. For bis-GMA, $\epsilon = 4.2$ and $\delta = 0.119$, for alumina $\epsilon = 9.0$ and $\delta = 0.0002$. The alumina does not absorb the microwave energy, and there is less bis-GMA present, therefore the temperature rise profile should be different from that for bis-GMA alone.

FUTURE WORK

Future work should include a detailed study of composite material in microwave. The differences in the temperature rise for resin alone versus that of the composite indicate that the composite filler has a significant impact on the reaction.

Experimental work by Park and Robertson [27] indicates that dipole interaction of 60 Hz AC fields and filler material gives organized structure to the composite material by aligning the composite filler particles, improving strength results. A hybrid approach where a composite material is heat cured while being exposed to low levels of microwave energy could verify if Park and Robertson's results are valid for 2.45 GHz.

The initiator is chosen depending on the method of cure desired. The resin studied in this work was formulated specifically for thermal curing. Typically benzoyl peroxide is used in thermal curing, and camphoroquinone is used for light curing. Research could focus on identifying an appropriate initiator for microwave applications.

REFERENCES

- [1] Annusavice, Phillips' Science of Dental Materials, 10th edition, WB Saunders Co., Philadelphia, PA, 1996, page 213
- [2] Annusavice, page 273
- [3] Annusavice, page 1
- [4] Annusavice, page 218,
- [5] Annusavice, page 214,
- [6] Annusavice, page 228,
- [7] Yau, W., Cheng, Y., Clark R., and Chow T., Pressure and temperature changes in heat-cured acrylic resin during processing., Dental Materials 18 (2002) 622-629
- [8] Jancar, J., Wang, W., DiBenedetto, A., Morphogenesis of tetrafunctional bis-GMA/TEGDMA Networks, Institute of Materials Science, University of Connecticut, Storrs, CT 06269-3136, U.S.A.
- [9] Arikawa, Fujii, Kanie, Inoue, Light transmittance characteristics of light cured composite resins, Journal of Dental Materials 14:405-411, November 1998
- [10] Silikas, Eliades, and Watts, Light intensity effects on resin-composite degree of conversion and shrinkage strain., Journal of Dental Materials 16 (2000) 292-296, January 2000.
- [11] Discussion with Dr. Ivan Stangel of Biomat Sciences on 21 August 2002.
- [12] Annusavice, Chapter 10
- [13] Boyd, The Science of Polymer Molecules, Cambridge University Press, Cambridge, UK, 1993, Chapter 1

- [14] Lovell, Lu, Elliot, Stansbury, and Bowman, The effect of cure rate on mechanical properties of dental resins, *Journal of Dental Materials* 17 (2001) 504-511, 2001.
- [15] Kelly, Perspectives on Strength, *Journal of Dental Materials* 11:103-110, 1995.
- [16] Brosh, Ganer Belov, Pilo, Analysis of strength properties of light-cured resin composites, *Journal of Dental Materials* 15 (1999) 174-179, December 1998.
- [17] Musanje, and Darvell, Polymerization of resin-composite restorative materials: exposure reciprocity, *Journal of Dental Materials* 19 (2003) 531-541, 2002.
- [18] Young, *University Physics*, 8th Edition, Addison-Wesley Publishing Company, Reading, MA, 1992, Chapter 15
- [19] Chen, and Barker, Effect of pressure on heat transport in polymers used in dentistry. *J. Biomed. Mater. Res.*, 6(3):147-154, 1972.
- [20] Doctors, and Carter, Thermal properties of non- metallic dental restoratives. Microfilmed Paper No. 163. [Delivered at] the annual meeting of the International Association for Dental Research, Dental Materials Group, Chicago, Illinois, March 18-21, 1971.
via http://www.lib.umich.edu/dentlib/Dental_tables/toc.html
- [21] Halvorson, Erickson, and Davidson, Energy dependent polymerization of resin based composite, *Journal of Dental Materials* 18 (2002) 463-469, 2002.
- [22] Ramo, Whinnery, and Van Duzer, *Fields and Waves in Communications Electronics*, 3rd Edition, Wiley and Sons, New York, NY, 1994.
- [23] Jackson, *Classical Electrodynamics*, 3rd Edition, Wiley and Sons, New York, NY, 1998.

- [24] Bartoloni, Murchison, and, Wofford, Degree of conversion in denture base materials for varied polymerization techniques, *Journal of Oral Rehabilitation*, Volume 27, Issue 6, June 2000.
- [25] Tam, Pulver, McComb, and,Smith, Physical properties of proprietary light-cured lining materials. *Oper. Dent.* 16:210-217, 1991
- [26] Smith, Powers, and Ladd, Mechanical properties of new denture resins polymerized by visible light, heat, and microwave energy. *Int. J. Prosthodont.* 5:315-320, 1992.
- [27] Park, and Robertson, Mechanical properties of resin composites with filler particles aligned by an electric field. *Journal of Dental Materials* 14:385-393, June 1998.